Brief Communication

MOLECULAR METABOLISM

Single nuclei RNA sequencing of the rat AP and NTS following GDF15 treatment

Benjamin C. Reiner [1,*], Richard C. Crist [1], Tito Borner [1,2], Robert P. Doyle [3], Matthew R. Hayes [1,2], Bart C. De Jonghe [1,2,]**

ABSTRACT

Objective: Growth differentiation factor 15 (GDF15) is known to play a role in feeding, nausea, and body weight, with action through the GFRAL-RET receptor complex in the area postrema (AP) and nucleus tractus solitarius (NTS). To further elucidate the underlying cell type-specific molecular mechanisms downstream of GDF15 signaling, we used a single nuclei RNA sequencing (snRNAseq) approach to profile AP and NTS cellular subtype-specific transcriptomes after systemic GDF15 treatment.

Methods: AP and NTS micropunches were used for snRNAseq from Sprague Dawley rats 6 h following GDF15 or saline injection, and Seurat was used to identify cellular subtypes and cell type-specific alterations in gene expression that were due to the direct and secondary effects of systemic GDF15 treatment.

Results: Using the transcriptome profile of ~35,000 individual AP/NTS nuclei, we identified 19 transcriptomically distinct cellular subtypes, including a single population *Gfral* and *Ret* positive excitatory neurons, representing the primary site of action for GDF15. A total of ~600 cell type-specific differential expression events were identified in neurons and glia, including the identification of transcriptome alterations specific to the direct effects of GDF15 in the *Gfral-Ret* positive excitatory neurons and shared transcriptome alterations across neuronal and glial cell types. Downstream analyses identified shared and cell type-specific alterations in signaling pathways and upstream regulatory mechanisms of the observed transcriptome alterations.

Conclusions: These data provide a considerable advance in our understanding of AP and NTS cell type-specific molecular mechanisms associated with GDF15 signaling. The identified cellular subtype-specific regulatory mechanism and signaling pathways likely represent important targets for future pharmacotherapies.

Keywords Area postrema; Nucleus of the solitary tract; GDF15; GFRAL; RET

1. INTRODUCTION

Growth differentiation factor 15 (GDF15), formerly known as macrophage inhibitory cytokine-1 (MIC-1), is a cytokine expressed and secreted in response to a variety of stimuli as part of stress and disease processes [1—4]. Clinical studies demonstrate that GDF15 levels serve as a biological marker for prognosis and diagnosis of certain types of cancers [5—8] and chronic hyperglycemia [9,10]. Importantly, exogenous GDF15 administration and increased endogenous GDF15 production (e.g., tumor-derived) suppress feeding and body weight primarily via the induction of nausea, emesis, and malaise [11,12].

The receptor for GDF15 remained elusive for years, but studies in mice treated with GDF15 provided evidence of a central neural network engaged by the cytokine, with GDF15-induced elevations in c-Fos expression observed in the area postrema (AP) and nucleus tractus solitarius (NTS) [13,14]. While the neuronal phenotypes within the AP and NTS are extremely heterogenous, emerging literature [11,15—19] highlights a small subset of neurons that express the glial-cell-derived neurotrophic factor (GDNF) family receptor alpha-like (GFRAL) receptor and RET coreceptor as the sole central substrate mediating GDF15's effects on anorexia and nausea/emesis [11,12]. Among the many shared neural substrates and anatomical nodes within the brain controlling various physiological functions, the hindbrain AP and NTS represent two contiguous nuclei involved in the regulation of energy balance, mediation of nausea/emesis, and indirect regulation of gastrointestinal motility [20,21]. Given the anomalous scenario whereby a small subset of neurons restricted to one region of the brainstem is driving such profound effects on body weight regulation and nausea/emesis elicited by a host of disease-driven elevations in GDF15 signaling, there is an urgent need to better understand the phenotype of these neurons. As GDF15 signaling becomes increasingly linked to the progression of diseases, including cancer, obesity, cachexia, uncontrolled nausea/vomiting, and cardiovascular disease [22—25], understanding the transcriptomic changes elicited by GDF15 in not only GFRAL and RET-coexpressing neurons, but also the second

[1]Department of Psychiatry, University of Pennsylvania, Philadelphia, PA 19104, USA [2]Department of Biobehavioral Health Sciences, University of Pennsylvania, Philadelphia, PA 19104, USA [3]Syracuse University, Department of Chemistry, 111 College Place, Syracuse, NY 13244, USA

*Corresponding author. TRL Building, 125 South 31st Street, Philadelphia, PA 19104, USA. E-mail: bcreiner@pennmedicine.upenn.edu (B.C. Reiner).

**Corresponding author. TRL Building, 125 South 31st Street, Philadelphia, PA 19104, USA. E-mail: bartd@nursing.upenn.edu (B.C. De Jonghe).

Received November 5, 2021 • Revision received November 30, 2021 • Accepted December 16, 2021 • Available online 21 December 2021

https://doi.org/10.1016/j.molmet.2021.101422

Abbreviations:

AP	Area postrema
Avg. Exp.	Average expression level of the gene
CholNeuro	Cholinergic Neurons
DEG	Differentially expressed genes
DMV	Dorsal motor nucleus of the vagus
DVC	Dorsal vagal complex
ExNeuro	Excitatory neurons
GDF15	Growth differentiation factor 15
GDNF	Glial-cell-derived neurotrophic factor
GEO	Gene expression omnibus
GFRAL	Glial-cell-derived neurotrophic factor family receptor alpha-like receptor
GO	Gene ontology
GWAS	Genome-wide association study
InNeuro	Inhibitory neurons
IPA	Ingenuity pathway analysis
LPBN	Lateral parabrachial nucleus
MIC-1	Macrophage inhibitory cytokine-1
MsigDB	Molecular and signatures database
NTS	Nucleus tractus solitarius
Oligodendro	Oligodendrocytes
OPC	Oligodendrocyte precursor cells
PC	Principal components
Pct. Exp.	Percentage of cells expressing the gene
PVN	Paraventricular nucleus
snRNAseq	Singe nuclei RNA sequencing
Ttr	Transthyretin
UMAP	Uniform manifold approximation and projection

order transcriptome alterations in other cells in the AP and NTS is imperative for the development of future therapeutics.

Recently, publications using genome-wide association studies (GWAS) [26] in humans and bulk or single nucleus RNA sequencing (snRNAseq) of the dorsal vagal complex (DVC; collectively comprised of the AP, NTS and dorsal motor nucleus of the vagus (DMV)) in mice [27–29], have illustrated or suggested connections between specific cell types within the AP and NTS controlling an intersection of emetic and energy balance circuits. Recent reports from murine AP and NTS tissue show that both neurons and supportive cells, as well as those cells expressing *Gfral*, *Gipr*, *Glp-1*, and *Calcr*, have distinct transcriptional profiles and exhibit differential expressed genes (DEGs) in relation to metabolic state [27–29]. The aforementioned reports all used mouse models, and there are important species differences at the level of the hindbrain in rats and mice with respect to expression and potential pathways governing these peptide system responses (see [30–32] for reviews). No detailed snRNAseq analysis of the AP and NTS has been performed in response to GDF15 signaling.

The current study highlights the DEGs associated with systemic GDF15 treatment in *Gfral* and *Ret* dual positive excitatory neurons and the second-order DEGs in other cells in these brainstem regions, in addition to providing an in-depth cell type-specific phenotypic profiling of gene expression in the Sprague–Dawley rat AP/NTS. snRNAseq data were generated and analyzed using known markers of major cell types, both neuronal and non-neuronal, within the AP and NTS of rats. We report specific focus of characterization and analysis of cell type-specific transcriptome alterations in an identified *Gfral* and *Ret* coexpressing excitatory neuronal cluster, as well as other cell types in the NTS and AP. We also present data identifying cell type-specific related GWAS phenotypes, affected canonical pathways and gene ontologies, and predicted upstream regulators of the observed differential expression.

2. MATERIALS AND METHODS

2.1. Animals, treatments, and tissue sampling

Adult male Sprague–Dawley rats (Charles River) weighing ~400 g were individually housed in hanging wire-bottomed cages under a 12 h:12 h light/dark cycle in a temperature- and humidity-controlled vivarium, with *ad libitum* access to water and chow (Purina Lab Diet 5001). Rats were daily handled and trained for intraperitoneal injections for a week prior to the experiment. Shortly before dark-onset, weight-matched rats were injected with either GDF15 or vehicle ($n = 4$, each). Recombinant human GDF15 (cat. 4569, Biovision) was dissolved in saline solution (5 mM Acetate salt, 240 mM Propylene Glycol and 0.007% Polysorbate 20, pH 4), and injected intraperitoneally at 100 μg/kg (1 mL/kg of body weight). The dose of GDF15 and time point were based on our prior work and selected to maximize anticipated transcriptome alterations [11,12]. Six hours after injections, rats were sedated using a cocktail of ketamine, xylazine, and acepromazine (180 mg/kg, 5.4 mg/kg and 1.28 mg/kg, respectively) in the middle of the dark-phase. Brains were removed and snap frozen in dry ice-cold hexane. Three adjacent micro-punch samples (each 1 cubic mm) containing the AP and bilateral NTS were collected from coronally-prepared brains on a cryostat, pooled together, and stored at −80 °C until processing similar to prior description [33]. All animal procedures were approved by the Institutional Animal Care and Use Committee of the University of Pennsylvania.

2.2. Nuclei isolation, library preparation, and sequencing

Frozen AP and NTS punches were used to prepare nuclei suspensions, similar to our previous description [34]. Pooled AP and NTS (AP/NTS) punches from each animal were homogenized in 500 μL of lysis buffer (Nuclease-free water with 10 mM Tris–HCL, 10 mM NaCl, 3 mM $MgCl_2$, 0.5% NP-40), diluted with an additional 2.5 mL of lysis buffer, allowed to rest of ice for 5 min, and further diluted with 3 mL of wash buffer (1X PBS with 2% BSA, 1:1000 RNase inhibitor, 0.25% Glycerol). Nuclei suspensions were passed through a 30 μm cell strainer to remove debris, pelleted by centrifugation, and resuspended three times. Nuclei were resuspended in wash buffer at 1,000 nuclei/μL. Nuclei suspensions were loaded onto the 10x Genomics microfluidic controller at 20,000 per sample, for a target capture of ~10,000 per sample. Sequencing libraries were produced with the 3′ Gene Expression Kit v3.1 according to the manufacturer's protocols. Libraries for all samples were pooled at equimolar concentrations and sequenced on a single NovaSeq 6000 S4 flow cell. Sequencing data were demultiplexed and aligned to the pre-mRNA reference rat transcriptome (Rnor6.0.101) using CellRanger v3.1.0.

2.3. Quality control, clustering, and annotation

Filtered read count matrixes for all samples were merged with Seurat v3.1. Nuclei with low numbers of detected genes (<528; ~0.5%) were considered low quality and removed due to likely being uninformative, similar to prior reports [35–38]. Nuclei in the top 0.5% of gene count (>4,947) and/or top 1% of UMI count (>11,376) were removed as putative multiplets, also similar to previous reports [35,37–39]. As previously detailed, nuclei with >5% of transcripts of mitochondrial origin were removed, and all mitochondrial transcripts were removed from the data set [40].

Counts were normalized to 10,000 counts per subject and scaled in Seurat. Variably expressed genes were identified with the FindVariableFeatures function, using the mean.var.plot selection method and analyzing only genes with mean scaled expression between 0.003 and 2. These parameters identified 1,165 highly variable genes, which were used to generate principal components (PCs). Clustering was performed using the first 50 PCs, generating 27 clusters at a resolution of 0.30. Six clusters were represented in only 4 of the 8 samples, with three of these clusters expressing *Slc17a7* (VGLUT1), a gene that is not present in the AP or NTS. These six clusters likely represent capture of adjacent brain stem nuclei (e.g., the DMX) and were removed from further analysis. In addition, ~90% of nuclei from one GDF15-treated animal originated from the six removed clusters and that sample was therefore removed from the data set. The remaining data were re-normalized, re-scaled, and clustered at 0.25 resolution. A single cluster was removed for low average UMI, leaving 21 clusters.

Major cell types were identified using known markers of major cell types [36]: Microglia: *Cx3cr1*, *Mrc1*; Endothelial — *Cldn5*; Astrocytes — *Cldn10*, *Glul*, *Aqp4*; Oligodendrocyte Precursor Cells (OPC) — *Pcdh15*, *Pdgfra*, *Olig1*, *Olig2*; Oligodendrocytes (Oligodendro) — *Mag*, *Mog*, *Plp1*, *Mobp*, *Mbp*; Excitatory Neurons (ExNeuro) — *Slc17a6*; Inhibitory Neurons (InNeuro) — *Gad1*, *Gad2*, *Slc32a1*; Cholinergic Neurons (CholNeuro) — *Slc5a7*; Neurons in general — *Snap25*, *Stmn2*; Tanycytes — *Vim* [41]; Ependymocytes — *Cfap52*, *Vim* [41]; Radial Glia — *Notch2* [42], *Slc1a3* [43]. Two clusters with mixed major cell type markers were removed for a final total of 19 clusters.

2.4. Quantification and analysis

Differential gene expression analysis was performed in Seurat using a Wilcoxon rank sum test to compare expression between GDF15-treated and control rats within each cluster. Bonferroni correction based on the total number of genes in the data set was used to adjust for multiple testing. Corrected p-values < 0.05 were considered significant.

Canonical pathway and predicted upstream regulator analysis were conducted using Ingenuity Pathway Analysis (IPA) [44]. For each cluster with $\geq$10 DEGs, a list of DEG Ensembl IDs, raw p-values, corrected p-values, and $\log_2$ fold change was used to perform the Core Analysis function. P-values were calculated using a right-tailed Fisher's exact test and corrected for multiple testing using a Benjamini-Hochberg correction ($\alpha = 0.1$).

Identification of gene ontologies (GO), KEGG pathways, transcription factor targets, microRNA targets, and GWAS Catalog endophenotypes with overrepresentation of cluster-specific DEGs was analyzed using FUMA and data from the Molecular and Signatures Database (MsigDB) v7.0 [45] and GWAS Catalog. For all analyses, all genes, except the MHC region, Ensembl v92 were used for the gene background and all results were corrected for multiple testing using a Benjamini-Hochberg correction ($\alpha = 0.05$).

2.5. Data availability

Single nuclei RNA sequencing data are available at the NCBI gene expression omnibus (GEO) under accession numbers GSE167981 and GSE167991

3. RESULTS

3.1. Single nuclei RNA sequencing and identification of cell types

To better understand the effect of GDF15 on the transcriptome of cells in the AP/NTS, we performed snRNAseq using the 10x Genomics 3' gene expression assay on AP/NTS punches from rats sacrificed 6 h after an i.p. injection of GDF15 (100 μg/kg, n = 3) or saline (n = 4). Samples were sequenced to an average depth of ~298 million reads (Table S1). We initially identified ~18,800 putative nuclei per sample, with average medians of ~1,400 genes and ~2,400 UMI per nucleus (Table S1). The number of sequencing reads per sample, number of nuclei per sample, average sequencing reads per nuclei per sample, median genes per nuclei per sample, and median UMI per nuclei per sample were consistent between the GDF15 and control groups (all p-values >0.1, Table S1, Fig. S1). After stringent quality control, we identified 34,784 nuclei, 14,772 from GDF15-injected rats and 20,012 from control rats, and these nuclei were used for all further analysis. Unbiased clustering was used to identify transcriptomically-distinct cellular populations (Methods 2.3.), and 19 cellular clusters were identified (Figure 1A). Nuclei from the GDF15 and control groups were found throughout all clusters (Fig. S2A). Clusters were annotated for the expression of known cellular subtype markers and all major neural cell types were identified (Figure 1B). The contribution of individual samples to each cluster (Fig. S2B) and the proportion of major cell types detected did not differ appreciably between the GDF15 and control groups (Fig. S3C). Expression of transcripts for the GDF15 receptor *Gfral* and the coreceptor *Ret* were detected in various cell types (Figure 1C; red dots indicate nuclei with $\geq$1 transcript). Knowing that GDF15 signaling requires binding to the Gfral and Ret heterodimeric complex [46], and that neural cell types expressing this receptor complex would be a direct site of action of our systemic GDF15 treatment, we next sought to identify these cell types. Most nuclei with detected transcripts for both *Gfral* and *Ret* were limited to a single excitatory neuronal subtype (ExNeuro1, Cluster 5; Figure 1C), suggesting that the ExNeuro1 cellular subtype contains the heterodimeric GFRAL-RET receptor and will be the site of direct action for GDF15.

3.2. Differential gene expression induced by systemic GDF15 treatment

To identify alterations in gene expression in AP/NTS cell types induced by systemic GDF15 treatment, snRNAseq data for the GDF15 and saline treatment groups for each cell cluster were compared. We identified a total of 581 differential expression events in 345 unique DEGs (Bonferroni corrected p-value < 0.05, Table S2, Figure 2A). DEGs were detected in all 19 clusters, with 77.5% of differential expression events being upregulation and 22.5% downregulation (Table S3, Figure 2B). Similar numbers of DEGs were observed throughout the excitatory and inhibitory neuronal clusters, accounting for 40.4% of differential expression events, while little differential expression was observed in the cholinergic neuronal clusters (Table S3). Non-neuronal DEGs were concentrated in the Oligodendrocyte1, Astrocyte, and Microglia clusters (3 of 10 non-neuronal clusters), accounting for 83.2% of non-neuronal DEGs and 48.7% of DEGs overall (Table S3).

Of relevance to the direct actions of the systemic GDF15 treatment, the ExNeuro1 cluster had 41 DEGs (32 upregulated, 9 downregulated), with the remaining 537 differential expression events in the other cellular subtypes being due to the secondary neural effects of systemic GDF15. Herein, the term 'secondary' is used to describe the effects of systemic GDF15 and to delineate from the effects caused by direct cellular interaction with GDF15. Thirty-two of the 41 DEGs in the ExNeuro1 cluster are also differentially expressed in at least one other cellular subtype, with 9 DEGs unique to the ExNeuro1 cluster (*Arhgap26*, *Atf1*, *Atp11c*, *Baiap3*, *Bdnf*, *Fus*, *Micb*, *Rgd1311703*, *Sptb*; Figure 2C, Table S2). Having already determined that not all ExNeuro1 nuclei had transcripts of the GDF15 receptor *Gfral* (Figure 1C), differential expression between the *Gfral* positive ExNeuro1 nuclei and the

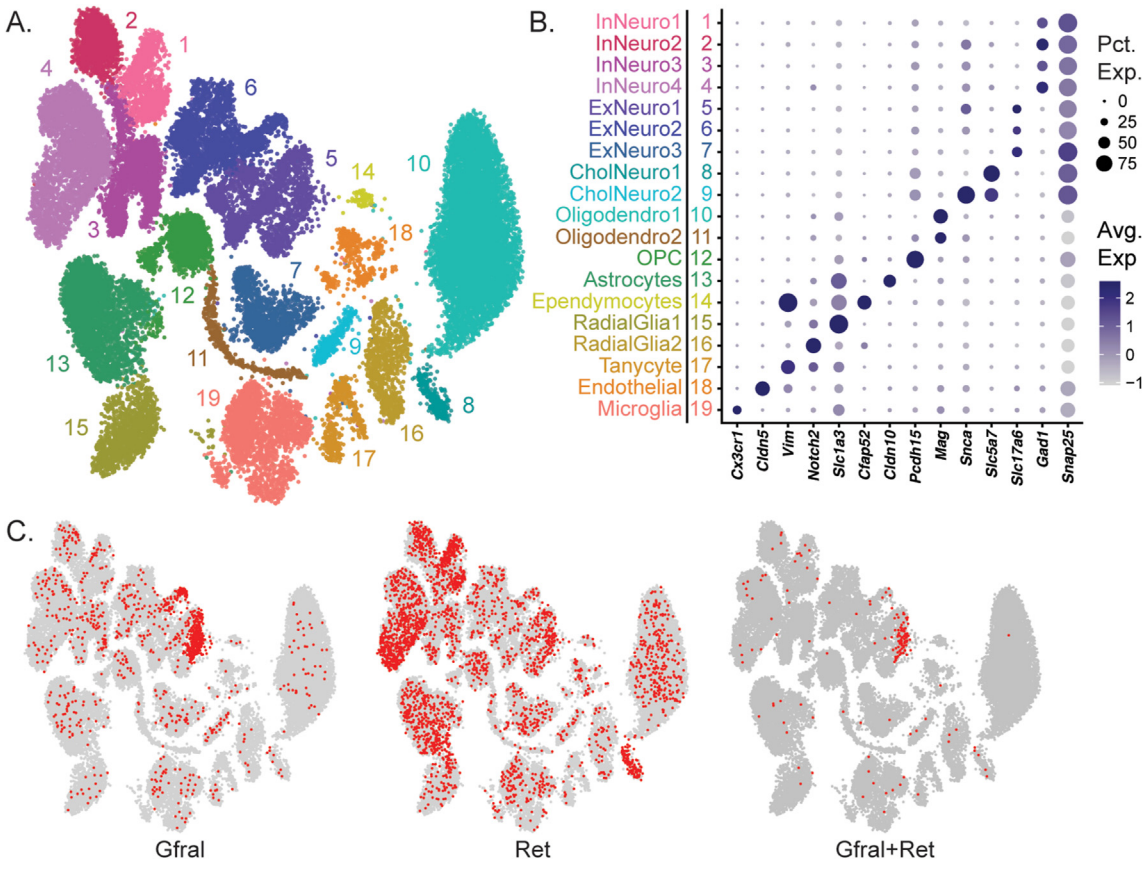

Figure 1: (A) Single nuclei RNA sequencing of rat AP and NTS identified 19 cellular subtypes, presented as a uniform manifold approximation and projection (UMAP) dimension reduction plot of all nuclei color coded by cluster. (B) Cluster were annotated for known marker genes for cellular subtypes in the AP and NTS. The size and color of dots are proportional to the percentage of cells expressing the gene (Pct. Exp.) and the average expression level of the gene (Avg. Exp.), respectively. The cluster numbers and colors are matched to that of the UMAP. (C) Highlighted UMAPs identifying nuclei containing transcripts for *Gfral*, *Ret*, or *Gfral* and *Ret*. The majority of nuclei with expression of both genes were from the ExNeuro1 cluster.

Gfral negative ExNeuro1 nuclei was examined. There were 16 DEGs identified in the analysis, including significant upregulation of the GDF15 coreceptor *Ret* [46] and *Dok5*, a component of the MAPK signaling cascade known to be activated by GDF15-Gfral signaling (see Table S4 for all DEGs). Taken together, these data provide face validity for the cell type specificity of our transcriptomic results.

3.3. Correlated patterns of gene expression

To understand how systemic GDF15 increase affected direct and secondary neurobiological mechanisms, we compared cluster-specific DEGs to GO terms (Table S5) and KEGG pathways (Table S6) to identify cell type-specific shared and unique neurobiological mechanisms for the *Gfral* and *Ret* coexpressing ExNeuro1 cluster and the other cell types of the AP/NTS. For example, the GO terms 'ION_TRANSPORT', 'CATION_TRANSPORT', and 'RESPONSE_TO_DRUG' were identified in multiple clusters, indicating a secondary effect to the systemic GDF15 treatment. Alternatively, seven GO terms related to amyloid beta formation, processing, and clearance were only identified in the *Gfral* and *Ret* coexpressing ExNeuro1 cluster (Table S5), indicating these are likely due to the direct action of GDF15. Shared and unique gene expression patterns in curated (Table S7) and computational (Table S8) gene sets from MSigDB were identified.

To identify metabolic and cell signaling pathways that are likely to be altered in response to systemic GDF15, canonical pathway analysis was performed with IPA using cluster specific DEGs. Shared and unique canonical pathways were identified for each cluster (Table S9). For example, LXR/RXR activation and FXR/RXR activation were both associated with nine clusters, corticotropin releasing hormone signaling with seven clusters (7/12), and maturity onset diabetes of young in four clusters. Overlap in identified cluster-specific canonical pathways was driven by shared DEGs (Table S9); for example, differential expression of *Apoe* and *Ttr* drove LXR/RXR activation and FXR/RXR activation association in all nine clusters. These results suggest that systemic GDF15 treatment induced shared alterations in metabolic and cell signaling pathways throughout cell types in the AP and NTS, not just those expressing *Gfral* and *Ret*.

3.4. Correlated patterns of expression regulation

To understand the regulatory mechanisms underlying the differential expression we observed for both the primary and secondary effects of systemic GDF15 treatment, cluster specific DEGs were utilized to identify putative cell type-specific regulators of differential expression. We identify microRNA (Table S10) and transcription factors (Table S11) with overrepresented targets amongst cluster-specific DEGs. For example, the transcription factors Stat5b, Tef1, and Mef2 had overrepresented targets amongst the *Gfral* and *Ret* coexpressing ExNeuro1 DEGs. While Stat5b was only predicted for the ExNeuro1 cluster, Tef1 and Mef2 were both predicted for four clusters. The overlap between

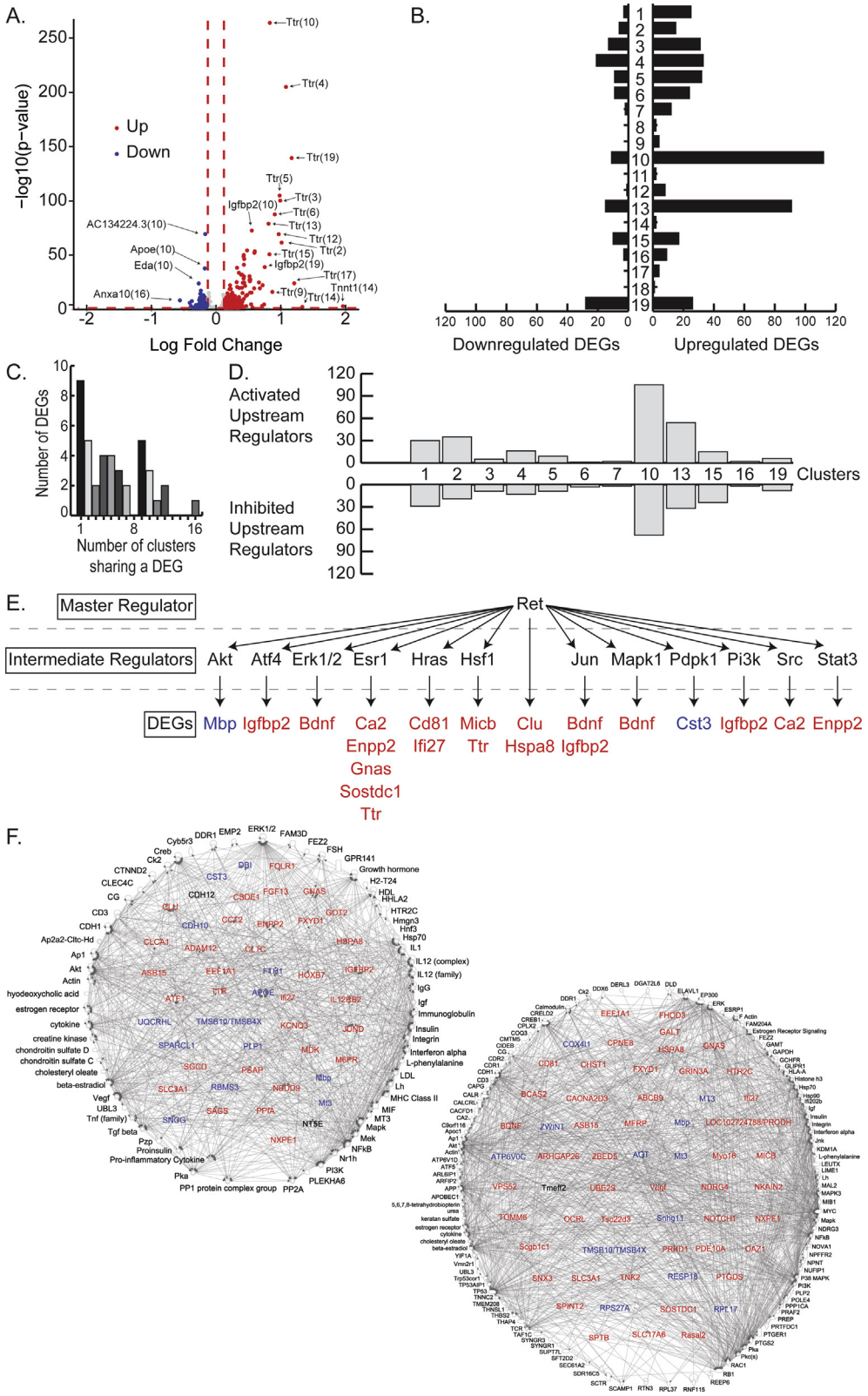

Figure 2: (A) A volcano plot depicting all significant differential expression events. Upregulated events are red and downregulated events are blue, and a subset of events are labeled with the gene symbol and number of the cluster in which it was significant (parentheses). (B) The number of upregulated or downregulated genes by cluster. (C) A histogram showing the number of clusters in which ExNeuro1 differential expressed genes (DEGs) were differential expressed. (D) The number of upstream regulators predicted to be activated or inhibited in each cluster. (E) A diagram showing the Ret modulated intermediate regulators that are predicted to control upregulate (red) and downregulated (blue) DEGs in the *Gfral* positive nuclei of the ExNeuro1 cluster. (F) Ingenuity Pathway Analysis identified two overlapping signaling networks that were shared by all seven excitatory and inhibitory neuronal clusters. Upregulated (red) and downregulated (blue) DEGs in the neuronal clusters are depicted in the center of each network and the connecting genes from the signaling networks are shown around the outside.

these putative regulators of cell type-specific differential expression suggests that systemic GDF15 treatment effects shared molecular mechanisms, while the identification of a unique transcription factor suggests a molecular mechanism distinct to the primary effects of systemic GDF15 treatment on cells in the ExNeuro1 cluster. These putative regulators of transcription act on differential expression directly. To identify both direct and indirect putative upstream regulators of the observed cell type-specific transcriptome alterations, IPA was used to predict activated and inhibited upstream regulatory network master regulators (Table S12, Figure 2D). IPA identified Ret as an activated upstream regulator of ExNeuro1 DEGs because 14 known regulators of ExNeuro1 DEGs were predicted to be activated and all 14 regulators are known to be activated by Ret activation (Table S12, Figure 2E). This predicted activation of Ret agrees with our observation that *Ret* expression was upregulated in *Gfral* expressing neurons in the ExNeuro1 cluster and suggests that the detected master regulators may be important in controlling systemic GDF15-induced transcriptome alterations. Our IPA analysis also identified two overlapping signaling networks that were shared by all seven excitatory and inhibitory neuronal clusters, further demonstrating shared neuronal mechanisms (Figure 2F).

3.5. Associations with GWAS phenotypes

We sought to determine if the primary or secondary effects of systemic GDF15 treatment on cell type-specific transcriptomes were similar to the genes previously associated with GWAS phenotypes. Cluster-specific DEGs were compared to the genes associated with GWAS Catalog phenotypes and overrepresentation was observed (Table S13). Overrepresentation of cluster specific DEGs amongst genes associated with a GWAS Catalog phenotypes was limited to glial cell clusters. These GWAS Catalog genes included loci that were previously associated with energy balance and metabolism, such as the microglia cluster being associated with GWAS loci for waist-hip ratio (DEGs: *Luzp2, Grin2b, Ly86, Ptprd*) and the astrocyte cluster being associated with GWAS loci for Type 2 diabetes (DEGs: *Camk2g, Slc1a2, Prkd1, Igfbp2, Zbtb20, Vegfa, Dgkb, Tnks*), fasting plasma glucose (DEGs: *Lrrtm4, Dgkb, Kank1*), and waist circumference adjusted for body mass index (DEGs: *Jund, Vegfa, Dgkb, Itgb8, Trpm3*). Taken together, these data suggest that these cell types in the AP/NTS might be associated with the endogenous alterations in GDF15 associated with these GWAS phenotypes.

4. DISCUSSION

The current study utilized a snRNAseq approach to examining both the primary and secondary effect of systemic GDF15 treatment on the transcriptome of the AP and NTS in the rat hindbrain. We believe these data to be critical to the field, as previous publications examining single nuclei transcriptomics in the AP and NTS have: 1) been limited thus far to mice [28,29], and 2) to date have made no assessment on the alterations induced by GDF15. We focused on the AP/NTS as nuclei of relevance to the processing of emetic and energy balance signals, like GDF15, and avoided the confounds of transcriptomic analyses in adjacent nuclei (i.e., DMV cells) that were previously reported in mice [28]. Our cluster analyses represent tissue captured from the dorsal AP and NTS at the rostral-to-caudal level of the AP and do not include the DMV. The data provide strong evidence that the *Gfral* and *Ret* expressing excitatory neuron population representing the primary neuronal cite of action for GDF15 is limited to a single excitatory neuronal subtype (see ExNeuro1, Figure 1C).

To identify both primary and secondary effects of the GDF15 treatment on cell type-specific transcriptomes, we characterized differential expression in *Gfral* and *Ret* expressing ExNeuro1 cluster, as opposed to a much broader population of cells that express Gfral alone without Ret (Figure 1C), and all other cell clusters, respectively. We report that GDF15 induces cell-type specific transcriptome alterations in 345 unique DEGs with greater than 75% of this differential expression being upregulation. Transthyretin (*Ttr*) expression was the most prominently upregulated DEG in our analysis of GDF15 vs. vehicle treated rats, across multiple neuronal and non-neuronal clusters, including the *Gfral* and *Ret* coexpressing ExNeuro1 cluster.

Ttr is most commonly associated with the transport of retinol and thyroxine within the periphery (i.e. blood) and cerebrospinal fluid [47]; however, *Ttr* expression in the hypothalamus in Sprague Dawley rats has been reported to play a functional role in modulating food intake and body weight [48]. Given our data, we postulate that changes in *Ttr* expression in the NTS and AP driven by GDF15 administration may be a contributing factor to the profound anorexia seen with Gfral-Ret activation. *Ttr* expression was not only upregulated in *Gfral-Ret* positive neurons, but also showed a dramatically upregulated expression in nearly every cell type in the AP/NTS (Figure 2A), suggesting a second-order GDF15-mediated event cascade downstream of Gfral-Ret-neuronal activation. Given the known role of Ttr in transporting thyroxine and that evidence demonstrates that very few *Gfral*-expressing neurons project to the paraventricular nucleus (PVN) [49], it is interesting to speculate that perhaps the brainstem Gfral-Ret neurons projecting to the lateral parabrachial nucleus (LPBN), which may consequently send afferents to the PVN to engage the HPA axis in a potent fashion. Collectively, such a hypothetical polysynaptic pathway could contribute to broad stress-mediated events linked with thyroxine and *Ttr* expression. A recent report shows both exogenous and endogenous GDF15 to be a potent agonist of the HPA axis [50]. As Ttr has also been considered to be a biomarker of oxidative stress [51], it is possible that Ttr may be a marker of GDF15-induced oxidative damage within the hindbrain as part of a downstream HPA axis response inducing sickness behavior and contributing to a broader CNS-wide anorectic circuit activation, although this notion requires further investigation.

The Gfral-Ret cluster exhibited increased *Igfbp2* expression and decreased *Apoe* expression. Insulin-like growth factors play regulatory roles in neural growth and development [52], Igf2 is ubiquitous in presence and roles, most notably in potential oncogenic signaling, perhaps as a biomarker of insulin resistance and CVD risk within the scope of metabolic disturbances [53]. However, while we find this discovery to be clearly of relevance to metabolic homeostasis, we do not know how Gfral-Ret activation may be linked directly to increased *Igfbp2* expression. The decrease in *Apoe* expression in the AP/NTS of GDF15-treated rats is consistent with a report showing intracerebroventricular Apoe injection reduced food intake through central melanocortin mechanisms within hypothalamic circuits [54]. Overexpression of GDF15 in macrophages in *Apoe* KO mice has been shown to influence atherosclerosis severity, although the mechanistic connection and directionality of effect between Apoe and GDF15 is also not clear [55]. Our canonical pathway analysis using cellular subtype specific DEGs showed differential expression of *Apoe* and *Ttr* drove LXR/RXR activation and FXR/RXR activation association in all nine clusters tested, suggesting that systemic GDF15 treatment induced shared alterations in metabolic and cell signaling pathways throughout cell types in the AP and NTS likely implicated in energetic and metabolic control. We identified Ret as an activated upstream regulator of ExNeuro1 DEGs (Table S11, Figure 2C), and this predicted *Ret* activation agreed with the observed increase in *Ret* expression in *Gfral* positive ExNeuro1 cluster

nuclei. Taken together, these results suggest that the identified intermediate regulators of differential expression could represent important therapeutic targets for modulating the effects of GDF15. The observation that astrocytes were enriched for differential expression of GWAS genes associated with obesity and metabolic disorder related phenotypes suggests that that the role of these genes in astrocytes may warrant future investigations. These data suggest that systemic GDF15 treatment induced both shared and cell type-specific mechanisms of transcriptome alteration. Translating these findings forward, it seems prudent to examine whether Ttr, Apoe, LXR and FXR can be targeted in the context of treating GDF15-related cachexia and nausea/emesis. It may be that some of the physiological responses to GDF15 (e.g., anorexia) can be retained while potentially mitigating other unwanted GDF15-mediated events, like nausea/emesis and activation of the HPA axis.

5. CONCLUSION

This work provides initial insight into the effects of GDF15 on cell type-specific transcriptomes, specifically the AP and NTS. GDF15 directly induced transcriptome alterations in a distinct population of *Gfral* and *Ret* expressing excitatory neurons, while the secondary effects of the systemically increased GDF15 induced broad upregulation and downregulation of identified DEGs within many cell types in the AP and NTS. The observed patterns in differential expression provide important information into the cell type-specific downstream signaling pathways that are altered by increased levels of GDF15, while the observed patterns in expression regulation further elucidates the molecular mechanisms controlling GDF15-induced transcriptome alterations. The identified cell type-specific DEGs, signaling pathways, regulatory mechanisms, and GWAS phenotypes further our understanding of the role of GDF15 in food intake, energy balance, illness-like behaviors, and metabolism, collectively providing important directions for future investigations and pharmacotherapies.

ACKNOWLEDGEMENTS

Supported by NIH-NIDDK R01 DK130239 (BCDJ, MRH, RPD) and R01 DK112812 (BCDJ).

CONFLICT OF INTEREST

None declared.

APPENDIX A. SUPPLEMENTARY DATA

Supplementary data to this article can be found online at https://doi.org/10.1016/j.molmet.2021.101422.

REFERENCES

[1] Bauskin, A.R., Brown, D.A., Kuffner, T., Johnen, H., Luo, X.W., Hunter, M., et al., 2006. Role of macrophage inhibitory cytokine-1 in tumorigenesis and diagnosis of cancer. Cancer Research 66(10):4983–4986.

[2] Tsai, V.W.W., Husaini, Y., Sainsbury, A., Brown, D.A., Breit, S.N., 2018. The MIC-1/GDF15-GFRAL pathway in energy homeostasis: implications for obesity, cachexia, and other associated diseases. Cell Metabolism 28(3):353–368.

[3] Staff, A.C., Bock, A.J., Becker, C., Kempf, T., Wollert, K.C., Davidson, B., 2010. Growth differentiation factor-15 as a prognostic biomarker in ovarian cancer. Gynecologic Oncology 118(3):237–243.

[4] Mullican, S.E., Rangwala, S.M., 2018. Uniting GDF15 and GFRAL: therapeutic opportunities in obesity and beyond. Trends in Endocrinology and Metabolism 29(8):560–570.

[5] Brown, D.A., Ward, R.L., Buckhaults, P., Liu, T., Romans, K.E., Hawkins, N.J., et al., 2003. MIC-1 serum level and genotype: associations with progress and prognosis of colorectal carcinoma. Clinical Cancer Research 9(7):2642–2650.

[6] Skipworth, R.J., Deans, D.A., Tan, B.H., Sangster, K., Paterson-Brown, S., Brown, D.A., et al., 2010. Plasma MIC-1 correlates with systemic inflammation but is not an independent determinant of nutritional status or survival in oesophago-gastric cancer. British Journal of Cancer 102(4):665–672.

[7] Koopmann, J., Buckhaults, P., Brown, D.A., Zahurak, M.L., Sato, N., Fukushima, N., et al., 2004. Serum macrophage inhibitory cytokine 1 as a marker of pancreatic and other periampullary cancers. Clinical Cancer Research 10(7):2386–2392.

[8] Breit, S.N., Johnen, H., Cook, A.D., Tsai, V.W., Mohammad, M.G., Kuffner, T., et al., 2011. The TGF-beta superfamily cytokine, MIC-1/GDF15: a pleotrophic cytokine with roles in inflammation, cancer and metabolism. Growth Factors 29(5):187–195.

[9] Adela, R., Banerjee, S.K., 2015. GDF-15 as a target and biomarker for diabetes and cardiovascular diseases: a translational prospective. Journal of Diabetes Research 2015:490842.

[10] Bao, X., Borne, Y., Muhammad, I.F., Nilsson, J., Lind, L., Melander, O., et al., 2019. Growth differentiation factor 15 is positively associated with incidence of diabetes mellitus: the Malmo Diet and Cancer-Cardiovascular Cohort. Diabetologia 62(1):78–86.

[11] Borner, T., Shaulson, E.D., Ghidewon, M.Y., Barnett, A.B., Horn, C.C., Doyle, R.P., et al., 2020. GDF15 induces anorexia through nausea and emesis. Cell Metabolism 31(2):351–362 e355.

[12] Borner, T., Wald, H.S., Ghidewon, M.Y., Zhang, B., Wu, Z., De Jonghe, B.C., et al., 2020. GDF15 induces an aversive visceral malaise state that drives anorexia and weight loss. Cell Reports 31(3):107543.

[13] Johnen, H., Lin, S., Kuffner, T., Brown, D.A., Tsai, V.W., Bauskin, A.R., et al., 2007. Tumor-induced anorexia and weight loss are mediated by the TGF-beta superfamily cytokine MIC-1. Nature Medicine 13(11):1333–1340.

[14] Tsai, V.W., Manandhar, R., Jorgensen, S.B., Lee-Ng, K.K., Zhang, H.P., Marquis, C.P., et al., 2014. The anorectic actions of the TGFbeta cytokine MIC-1/GDF15 require an intact brainstem area postrema and nucleus of the solitary tract. PLoS One 9(6):e100370.

[15] Breit, S.N., Tsai, V.W., Brown, D.A., 2017. Targeting obesity and cachexia: identification of the GFRAL receptor-MIC-1/GDF15 pathway. Trends in Molecular Medicine 23(12):1065–1067.

[16] Emmerson, P.J., Wang, F., Du, Y., Liu, Q., Pickard, R.T., Gonciarz, M.D., et al., 2017. The metabolic effects of GDF15 are mediated by the orphan receptor GFRAL. Nature Medicine 23(10):1215–1219.

[17] Hsu, J.Y., Crawley, S., Chen, M., Ayupova, D.A., Lindhout, D.A., Higbee, J., et al., 2017. Non-homeostatic body weight regulation through a brainstem-restricted receptor for GDF15. Nature 550(7675):255–259.

[18] Mullican, S.E., Lin-Schmidt, X., Chin, C.N., Chavez, J.A., Furman, J.L., Armstrong, A.A., et al., 2017. GFRAL is the receptor for GDF15 and the ligand promotes weight loss in mice and nonhuman primates. Nature Medicine 23(10):1150–1157.

[19] Yang, L., Chang, C.C., Sun, Z., Madsen, D., Zhu, H., Padkjaer, S.B., et al., 2017. GFRAL is the receptor for GDF15 and is required for the anti-obesity effects of the ligand. Nature Medicine 23(10):1158–1166.

[20] Hesketh, P.J., 2008. Chemotherapy-induced nausea and vomiting. New England Journal of Medicine 358(23):2482–2494.

[21] Babic, T., Browning, K.N., 2014. The role of vagal neurocircuits in the regulation of nausea and vomiting. European Journal of Pharmacology 722:38–47.

[22] Jiang, W.W., Zhang, Z.Z., He, P.P., Jiang, L.P., Chen, J.Z., Zhang, X.T., et al., 2021. Emerging roles of growth differentiation factor-15 in brain disorders (Review). Experimental and Therapeutic Medicine 22(5):1270.

[23] Harlid, S., Gunter, M.J., Van Guelpen, B., 2021. Risk-predictive and diagnostic biomarkers for colorectal cancer; a systematic review of studies using pre-diagnostic blood samples collected in prospective cohorts and screening settings. Cancers 13(17).

[24] Meijers, W.C., Bayes-Genis, A., Mebazaa, A., Bauersachs, J., Cleland, J.G.F., Coats, A.J.S., et al., 2021. Circulating heart failure biomarkers beyond natriuretic peptides: review from the biomarker study group of the heart failure association (HFA), European society of cardiology (ESC). Eur J Heart Fail.

[25] Olson, B., Diba, P., Korzun, T., Marks, D.L., 2021. Neural mechanisms of cancer cachexia. Cancers 13(16).

[26] Wittekind, D.A., Scholz, M., Kratzsch, J., Loffler, M., Horn, K., Kirsten, H., et al., 2021. Genome-wide association and transcriptome analysis suggests total serum ghrelin to be linked with GFRAL. European Journal of Endocrinology 184(6):847—856.

[27] Dowsett, G.K.C., Lam, B.Y.H., Tadross, J.A., Cimino, I., Rimmington, D., Coll, A.P., et al., 2021. A survey of the mouse hindbrain in the fed and fasted states using single-nucleus RNA sequencing. Molecular Metabolism 53:101240.

[28] Ludwig, M.Q., Cheng, W., Gordian, D., Lee, J., Paulsen, S.J., Hansen, S.N., et al., 2021. A genetic map of the mouse dorsal vagal complex and its role in obesity. Nat Metab 3(4):530—545.

[29] Zhang, C., Kaye, J.A., Cai, Z., Wang, Y., Prescott, S.L., Liberles, S.D., 2021. Area postrema cell types that mediate nausea-associated behaviors. Neuron 109(3):461—472 e465.

[30] Cui, Q.N., Stein, L.M., Fortin, S.M., Hayes, M.R., 2021. The role of glia in the physiology and pharmacology of GLP-1: implications for obesity, diabetes, and neurodegenerative processes including glaucoma. British Journal of Pharmacology.

[31] Grill, H.J., Hayes, M.R., 2012. Hindbrain neurons as an essential hub in the neuroanatomically distributed control of energy balance. Cell Metabolism 16(3):296—309.

[32] Kanoski, S.E., Hayes, M.R., Skibicka, K.P., 2016. GLP-1 and weight loss: unraveling the diverse neural circuitry. American Journal of Physiology - Regulatory, Integrative and Comparative Physiology 310(10):R885—R895.

[33] Borner, T., Geisler, C.E., Fortin, S.M., Cosgrove, R., Alsina-Fernandez, J.A., Dogra, M., et al., 2021. GIP receptor agonism attenuates GLP-1 receptor agonist induced nausea and emesis in preclinical models. Diabetes.

[34] Reiner, B.C., Crist, R.C., Stein, L.M., Weller, A.E., Doyle, G.A., Arauco-Shapiro, G., et al., 2020. Single-nuclei transcriptomics of schizophrenia prefrontal cortex primarily implicates neuronal subtypes. bioRxiv.

[35] Mathys, H., Davila-Velderrain, J., Peng, Z., Gao, F., Mohammadi, S., Young, J.Z., et al., 2019. Single-cell transcriptomic analysis of Alzheimer's disease. Nature 570(7761):332—337.

[36] Nagy, C., Maitra, M., Tanti, A., Suderman, M., Theroux, J.F., Davoli, M.A., et al., 2020. Single-nucleus transcriptomics of the prefrontal cortex in major depressive disorder implicates oligodendrocyte precursor cells and excitatory neurons. Nature Neuroscience.

[37] Schirmer, L., Velmeshev, D., Holmqvist, S., Kaufmann, M., Werneburg, S., Jung, D., et al., 2019. Neuronal vulnerability and multilineage diversity in multiple sclerosis. Nature 573(7772):75—82.

[38] Velmeshev, D., Schirmer, L., Jung, D., Haeussler, M., Perez, Y., Mayer, S., et al., 2019. Single-cell genomics identifies cell type-specific molecular changes in autism. Science 364(6441):685—689.

[39] Nagy, C., Maitra, M., Tanti, A., Suderman, M., Theroux, J.F., Davoli, M.A., et al., 2020. Single-nucleus transcriptomics of the prefrontal cortex in major depressive disorder implicates oligodendrocyte precursor cells and excitatory neurons. Nature Neuroscience 23(6):771—781.

[40] Osorio, D., Cai, J.J., 2020. Systematic determination of the mitochondrial proportion in human and mice tissues for single-cell RNA sequencing data quality control. Bioinformatics.

[41] Zhang, C., Kaye, J.A., Cai, Z., Wang, Y., Prescott, S.L., Liberles, S.D., 2020. Area postrema cell types that mediate nausea-associated behaviors. Neuron.

[42] Mase, S., Shitamukai, A., Wu, Q., Morimoto, M., Gridley, T., Matsuzaki, F., 2020. Notch1 and Notch2 collaboratively maintain radial glial cells in mouse neurogenesis. Neurosciences Research.

[43] Pollen, A.A., Nowakowski, T.J., Chen, J., Retallack, H., Sandoval-Espinosa, C., Nicholas, C.R., et al., 2015. Molecular identity of human outer radial glia during cortical development. Cell 163(1):55—67.

[44] Kramer, A., Green, J., Pollard Jr., J., Tugendreich, S., 2014. Causal analysis approaches in ingenuity pathway analysis. Bioinformatics 30(4):523—530.

[45] Liberzon, A., Subramanian, A., Pinchback, R., Thorvaldsdottir, H., Tamayo, P., Mesirov, J.P., 2011. Molecular signatures database (MSigDB) 3.0. Bioinformatics 27(12):1739—1740.

[46] Rochette, L., Zeller, M., Cottin, Y., Vergely, C., 2020. Insights into mechanisms of GDF15 and receptor GFRAL: therapeutic targets. Trends in Endocrinology and Metabolism 31(12):939—951.

[47] Schreiber, G., Southwell, B.R., Richardson, S.J., 1995. Hormone delivery systems to the brain-transthyretin. Experimental and Clinical Endocrinology & Diabetes 103(2):75—80.

[48] Zheng, F., Kim, Y.J., Moran, T.H., Li, H., Bi, S., 2016. Central transthyretin acts to decrease food intake and body weight. Scientific Reports 6:24238.

[49] Worth, A.A., Shoop, R., Tye, K., Feetham, C.H., D'Agostino, G., Dodd, G.T., et al., 2020. The cytokine GDF15 signals through a population of brainstem cholecystokinin neurons to mediate anorectic signalling. Elife 9.

[50] Cimino, I., Kim, H., Tung, Y.C.L., Pedersen, K., Rimmington, D., Tadross, J.A., et al., 2021. Activation of the hypothalamic-pituitary-adrenal axis by exogenous and endogenous GDF15. Proceedings of the National Academy of Sciences of the U S A 118(27).

[51] Sharma, M., Khan, S., Rahman, S., Singh, L.R., 2019. The extracellular protein, transthyretin is an oxidative stress biomarker. Frontiers in Physiology 10:5.

[52] Dyer, A.H., Vahdatpour, C., Sanfeliu, A., Tropea, D., 2016. The role of Insulin-Like Growth Factor 1 (IGF-1) in brain development, maturation and neuroplasticity. Neuroscience 325:89—99.

[53] Heald, A.H., Kaushal, K., Siddals, K.W., Rudenski, A.S., Anderson, S.G., Gibson, J.M., 2006. Insulin-like growth factor binding protein-2 (IGFBP-2) is a marker for the metabolic syndrome. Experimental and Clinical Endocrinology & Diabetes 114(7):371—376.

[54] Shen, L., Tso, P., Woods, S.C., Clegg, D.J., Barber, K.L., Carey, K., et al., 2008. Brain apolipoprotein E: an important regulator of food intake in rats. Diabetes 57(8):2092—2098.

[55] Johnen, H., Kuffner, T., Brown, D.A., Wu, B.J., Stocker, R., Breit, S.N., 2012. Increased expression of the TGF-b superfamily cytokine MIC-1/GDF15 protects ApoE(-/-) mice from the development of atherosclerosis. Cardiovascular Pathology 21(6):499—505.

